

Journal of Biomedical Optics

SPIEDigitalLibrary.org/jbo

***In vivo* inflammation mapping of periodontal disease based on diffuse reflectance spectral imaging: a clinical study**

Chandra Sekhar Prasanth
Joseph Betsy
Jayaraj L. Jayanthi
Unni G. Nisha
Janam Prasantila
Narayanan Subhash

In vivo inflammation mapping of periodontal disease based on diffuse reflectance spectral imaging: a clinical study

Chandra Sekhar Prasanth,^a Joseph Betsy,^b Jayaraj L. Jayanthi,^c Unni G. Nisha,^a Janam Prasantila,^b and Narayanan Subhash^a

^aCentre for Earth Science Studies, Biophotonics Laboratory, PB No. 7720, Akkulam, Thiruvananthapuram, Kerala 695031, India

^bGovernment Dental College, Department of Periodontics, Thiruvananthapuram, Kerala 695 011, India

^cDivision of Surgical Oncology, Regional Cancer Center, Thiruvananthapuram, Kerala 695 011, India

Abstract. Since conventional techniques using periodontal probes have inherent drawbacks in the diagnosis of different grades of gingival inflammation, development of noninvasive screening devices becomes significant. Diffuse reflectance (DR) spectra recorded with white light illumination is utilized to detect periodontal inflammation from the oxygenated hemoglobin absorption ratio R620/R575. A multispectral imaging system is utilized to record narrow-band DR images at 575 and 620 nm from the anterior sextant of the gingiva of 15 healthy volunteers and 25 patients ($N = 40$). An experienced periodontist assesses the level of gingival inflammation at each site through periodontal probing and assigns diagnosis as healthy, mild, moderate, or severe inflammation. The DR image ratio R620/R575 computed for each pixel (8- μm resolution) from the monochrome images is pseudo-color-mapped to identify gingival inflammation sites. The DR image ratio values at each site are compared with clinical diagnosis to estimate the specificity and sensitivity of the DR imaging technique in inflammation mapping. The high diagnostic accuracy is utilized to detect underlying inflammation in six patients with a previous history of periodontitis.

© 2013 Society of Photo-Optical Instrumentation Engineers (SPIE) [DOI: 10.1117/1.JBO.18.2.026019]

Keywords: diffuse reflectance spectroscopy; periodontal disease; gingival inflammation; oxygenated hemoglobin; noninvasive detection of inflammation; electron multiplying charge coupled device camera.

Paper 12628PRR received Sep. 21, 2012; revised manuscript received Jan. 10, 2013; accepted for publication Jan. 22, 2013; published online Feb. 12, 2013.

1 Introduction

Periodontal diseases are infectious diseases that destroy the periodontal attachment apparatus, resulting in the loss of tooth support. The American Academy of Periodontology acknowledged recently that the development of enhanced surveillance and prognostic tools is essential for the control of periodontal diseases. Recent studies have revealed the association of periodontal disease with adverse pregnancy outcomes,¹ cardiovascular disease, stroke, pulmonary disease,^{2,3} and diabetes.⁴

Successful treatment of periodontal diseases depends on accurate diagnosis of sites with periodontal inflammation. At present, clinical diagnosis of periodontal inflammation is based almost entirely on the visual perception of tissue color and clinical probing. Accepted diagnostic practices include intraoral periapical (IOPA) X ray to estimate bone loss and clinical assessments, such as bleeding on probing (BOP) and gingival index (GI), to detect the presence of inflammation. Even though the trained physician's eye is a powerful tool, such evaluations are subjective and semiquantitative. Therefore, uniform criteria have not yet been established in periodontal disease diagnosis.⁵ Investigations into the pathogenesis of periodontal disease are often based on the role of bacterial infection. However, the host response factors, such as the immune and inflammatory responses, are critical to the pathogenesis of periodontal disease.⁶⁻⁸ It is known that the natural immune system activates local inflammatory reactions in response to bacterial infection.

In view of the inherent drawbacks with conventional diagnostic procedures, the development of novel noninvasive diagnostic techniques becomes significant.

Diffuse reflectance spectroscopy has been used in various studies to distinguish between healthy and malignant tissues. Subhash et al.⁹ proposed the use of the oxygenated hemoglobin absorption intensity ratio (R545/R575) for the classification of different grades of oral cancer by studying the DR spectral features of surgically excised tissues. In a later clinical study, Mallia et al.¹⁰ applied the DR ratiometric technique for *in situ* detection and discrimination of oral premalignant and malignant lesions. Further clinical studies using the DR spectral intensity ratio (R545/R575) confirmed the potential of this technique for detecting oral cancer with high sensitivity and specificity and discriminating oral precancers of the tongue and lip that are difficult to diagnose from tissue autofluorescence.^{11,12}

Accurate and objective documentation through imaging is often required to monitor the evolution of the gingival inflammation. A longitudinal study on dogs revealed that, during inflammation, the relative oxygenated and deoxygenated hemoglobin concentrations increased, while the oxygenation level decreased.¹³ These observations were later confirmed by the same group in a cross sectional study on humans to detect healthy and moderately inflamed cases.¹⁴ Taking advantage of the spectral properties of oxyhemoglobin (oxy-Hb) and deoxyhemoglobin (deoxy-Hb) in the visible part of the spectrum, Zonios et al.¹⁵ evaluated their apparent concentrations in the tissue by spectroscopic analysis of diffusely reflected light. Later, Stamatas and Kollias¹⁶ showed that erythema is linked to an

Address all correspondence to: Narayanan Subhash, Biophotonics Laboratory, Centre for Earth Science Studies, PB No. 7720, Akkulam, Thiruvananthapuram, Kerala 695031, India. Tel: +91 471 2511638; Fax: +91 471 2442280; Mob: 91-9400497015; E-mail: subhash@cess.res.in

increase in the apparent concentration of oxy-Hb, while accumulation of deoxy-Hb depends on blood stasis. Recent advances in digital imaging technology and optics have enabled the development of hyper-spectral imaging systems that can locate and identify cutaneous erythema, blanching, pigmentation, and induration.¹⁷

Recent reports by Liu et al.¹⁸ and Zili Ge et al.¹⁹ established the potential of optical spectroscopy to determine multiple inflammatory indices in periodontal tissues. DR imaging studies of periodontal disease by Zakian et al.²⁰ based on oxy-Hb and deoxy-Hb crossovers at 615 and 460 nm demonstrated that the image intensity ratio (R615/R460) could be utilized to discriminate between healthy and diseased sites of the periodontium. Recently, Sekhar et al.²¹ measured the DR spectra from the gingiva of 60 patients and 30 healthy volunteers with a miniature spectrometer using a fiber-optic probe with white light illumination. On examination of the diagnostic accuracies of various DR ratios, such as R620/R545, R615/R460, and R620/R575, it was observed that the R620/R575 ratio gives the best discrimination between different grades of gingival inflammation.

This clinical study explores the prospect of using the DR ratio R620/R575 to map periodontal disease *in vivo* by recording monochrome images of gingiva at 575 nm and at the peak of DR spectral emission (620 nm) using a highly sensitive electron multiplying charge coupled device (EMCCD) camera coupled to a tunable filter with a bandwidth of 7 nm. The image ratio R620/R575 was computed to discriminate various grades of gingival inflammation, and the diagnostic accuracies derived from the scatterplot of the image ratio show the potential of DR imaging to detect sites with subclinical disease and future disease progression.

2 Materials and Methods

2.1 Clinical Protocol

The study population consisted of a control group of 15 healthy volunteers with no clinical signs of gingival inflammation, a test group I of 25 patients with overt signs of gingival inflammation, and a test group II of six patients with a previous history of periodontitis but no overt signs of gingival inflammation (Table 1). The study was carried out at the out-patient clinic of the Government Dental College (GDC), Thiruvananthapuram, Kerala, India. The study protocol was approved by the GDC Institutional Ethical Committee (No. IEC/C/42-A/2011/DCT/

dated 18-01-2011). Every volunteer was informed about the nature of the study, and informed consent was obtained prior to initiation of any study-related measurements. The healthy volunteers and patients enrolled in the study were selected by an experienced periodontist. The patients enrolled in the test groups were 25 to 65 years old, whereas the healthy volunteers were 20 to 35 years old. The clinical study was conducted from April 2011 to November 2011.

The clinical parameters and treatment history of all participants were recorded. Healthy sites were defined as those with pocket depth (PD) <3 mm and no BOP. The healthy volunteers selected for participation had no clinical signs of gingival inflammation and maintained good oral hygiene. Spectral images of the gingival papillae from canine to canine in both the upper and lower arches (10 sites in total) were acquired from all participants.

All patients were categorized based on the GI, which was introduced by Loe and Silness in 1963. The GI scores of 0, 1, 2, and 3 were assigned as normal gingiva, mild inflammation (with slight change in color and slight edema) in 96 sites, moderate inflammation (redness, edema, glazing, and BOP) in 54 sites, and severe inflammation (marked redness, edema, ulceration, and spontaneous bleeding) in 17 sites, respectively. Test group I consisted of 16 patients with a GI score of 1 (96 sites), six patients with a GI score of 2 (54 sites), and three patients with a GI score of 3 (17 sites). Test group II had six patients (eight sites) with previous history of periodontitis but no overt signs of inflammation (Table 1).

The periodontal charts of these patients showed that they had PD \geq 5 mm with BOP.²² IOPA X ray of these sites was taken to check the presence of bone loss. In order to avoid overlap between healthy gingiva and mild disease conditions, patients with a PD of 3 to 4 mm were excluded. Other exclusion criteria applied in patient selection were:

1. Calculus index (simplified) score higher than 1.8
2. Anti-inflammatory medications (e.g., nonsteroidal anti-inflammatory drugs, steroids, antibiotics, or immunosuppressants) in the past three months
3. Any systemic condition, such as inflammatory diseases or diabetes, that may interfere with the study
4. Volunteers with a previous medical history of cardiovascular problems.

Table 1 Characteristics of the study group.

Selection criteria	Study groups	Age groups	No. of subjects	Total no. of sites
No clinical signs of gingival inflammation	Healthy (control) (GI-0)	20-35 years	15	90
With clinical signs of gingival inflammation	Test group I	Mild (GI-1)	16	96
		Moderate (GI-2)	6	54
		Severe (GI-3)	3	17
Attachment loss with earlier history of periodontitis and no overt signs of inflammation	Test group II	Periodontitis	6	8
		Total	46	265

2.2 Instrumentation

The diffuse reflectance imaging system shown in Fig. 1 consists of an EMCCD camera (Model: LUCA-R, DL-604M-OEM, Andor Technology, UK) with $1004 (H) \times 1002 (V)$ pixels, a Nikon AF 35-70 zoom camera lens, and a liquid crystal tunable filter (LCTF) with a bandwidth of 7 nm (Model: VIS-07-20-STD, CRI Inc., USA) that can be tuned electronically to any wavelength in the range of 400 to 720 nm. In this study, the LCTF was tuned to coincide with the oxy-Hb absorption peak at 575 nm and the DR spectral intensity maximum at 620 nm. The specifications of the EMCCD camera used for imaging is given in Table 2. Suitable adapters and roller assemblies were built to couple the camera with the focusing lens and LCTF and to facilitate camera lens movement during focusing and zooming. The tungsten halogen lamp (12 V, 55 W) of the dental chair (Trichur Surgicals, Kerala, India) was used for white light illumination of the oral cavity during imaging. Sequential recording of the DR images at 575 and 620 nm and computation of the image ratio R_{620}/R_{575} were controlled by the solutions for imaging and spectroscopy (SOLIS) program (Andor Technology, United Kingdom, Ver. 1.0) and LCTF control software.

2.3 Data Acquisition

The DRIS assembly was kept in the instrument tray of the dental chair at a distance of one foot from the patient for the easy imaging of the anterior sextant of the gingiva. A sterilized cheek retractor was used to pull the cheeks away from the mouth and hold them in place during camera exposure. The DR imaging was carried out in a dark room to keep external light from entering the camera. Before the tungsten halogen lamp was turned on, the patient was given an eye protective goggle to ensure comfort. The patients were asked to remain stationary for 20 s during the sequential acquisition of images at 620 and 575 nm with the LCTF control software. DR imaging was always performed before clinical assessments, because an injury of the blood vessels of the crevicular plexus by paper strips and a periodontal probe could affect the reflectance spectra of gingiva. Before taking DR measurements, saliva was removed from the gingiva with an absorbing tissue to reduce specular reflection

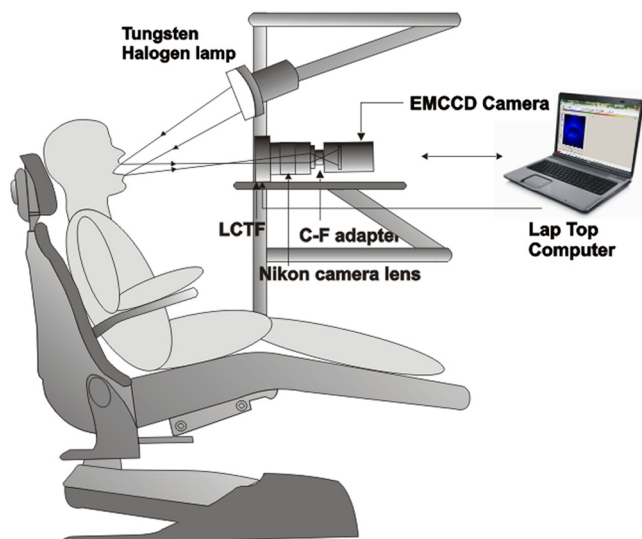


Fig. 1 Schematic of the experimental arrangement for *in vivo* DR imaging measurements.

Table 2 Specifications of EMCCD camera used for imaging of diffuse reflected light from periodontal region.

Active pixels ($H \times V$)	1004 \times 1002
Pixel size ($W \times H$; μm)	8 \times 8
Image area (mm)	8 \times 8
Quantum efficiency at 600 nm (%)	65
Cooling temperature ($^{\circ}\text{C}$)	-20
Electron multiplier gain	1 to 1000 times
Frame rate (frames per sec)	12.4
Active area pixel well depth (e^{-} , typical)	30,000
PC interface	USB 2.0

and increase light penetration, thereby enhancing the diffuse reflectance from underlying tissues.

The Andor SOLIS image capturing software that recorded the grayscale images of gingiva has a provision for carrying out automatic image alignment with pixel accuracy to compensate for slight patient/camera movement during imaging. Arithmetic functions associated with the software were used to compute the ratio images. A pseudo color map (PCM) of the image intensity ratio (R_{620}/R_{575}) variation was generated using the same software to distinguish clearly between healthy and diseased sites. Differences in the diffuse reflectance were calculated for every image pixel, approximately corresponding to the area occupied by a single cell. Properties such as the diffuse reflectance were calculated from the pixel intensity, and their spatial distribution (PCM) was overlaid on to the image of the diseased site. The PCM of the ratio image classified the gingiva as blue (healthy tissue), green (mild inflammation), red (moderate inflammation), or yellow/white (severe inflammation).

2.4 Spectral Data Processing

Region of interest (ROI) is an important post-acquisition tool for quantitative analysis of data using the Andor SOLIS program. Thirty ROIs with a maximum size of 100 pixels were selected for each site in the ratio images of patients and healthy subjects. Mean pixel intensity was estimated as the average of 30 such ROIs from each site. These intensity values are presented in a scatterplot diagram for tissue classification as healthy, mild, moderate, and severe.

2.5 Statistical Analysis

Summary statistics (proportion, mean, and SD) were used to describe the collected data. The study group was divided into four different categories (healthy gingiva, mild inflammation, moderate inflammation, and severe inflammation) based on GI value. Differences in mean age were compared across these three groups using analysis of variance (ANOVA). The medians of mean pixel intensities were compared across the study groups using Kruskal-Wallis one-way ANOVA (K samples) to discriminate healthy tissue from mild inflammation, healthy tissue from moderate inflammation, healthy tissue from severe inflammation, and moderate inflammation from severe inflammation.

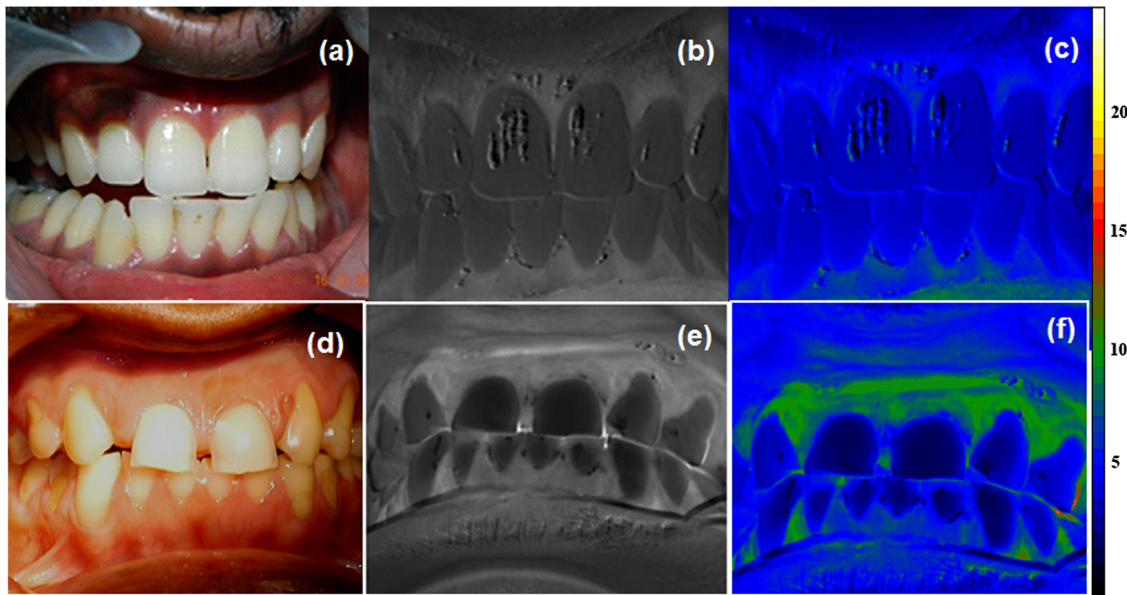


Fig. 2 (a) Healthy gingiva, (b) grayscale image ratio R620/R575 of healthy gingiva, (c) PCM ratio image of healthy gingiva, (d) gingiva with mild inflammation, (e) grayscale ratio image of gingiva with mild inflammation, and (f) PCM ratio image of gingiva with mild inflammation.

We used Statistical Package for Social Sciences (Ver. 17, SPSS, Inc., Chicago, Illinois) for all analyses.

3 Results

3.1 Image Analysis Features

Figures 2–4 show clinical photos of diseased periodontium, along with the monochrome and processed ratio images for healthy/mild, moderate, and severe inflammatory conditions, respectively. Figure 2(c) is the PCM R620/R575 ratio image

of a healthy volunteer, shown in Fig. 2(a); the corresponding grayscale ratio image is shown in Fig. 2(b). Figure 2(d) shows the photo of the gingiva of a patient with mild inflammation. The grayscale ratio (R620/R575) image for that patient, shown in Fig. 2(e), appears in green color after PCM in regions of mild inflammation, as shown in Fig. 2(f). Pseudo color code is also shown to denote pixel intensity variations.

The pseudo coloring of the monochromatic ratio image with varying pixel intensity helps to locate points of maximum oxy-Hb absorption. It can be seen that the average pixel intensity ratio value is 4.81 ± 1.04 for healthy tissue but 8.82 ± 1.79

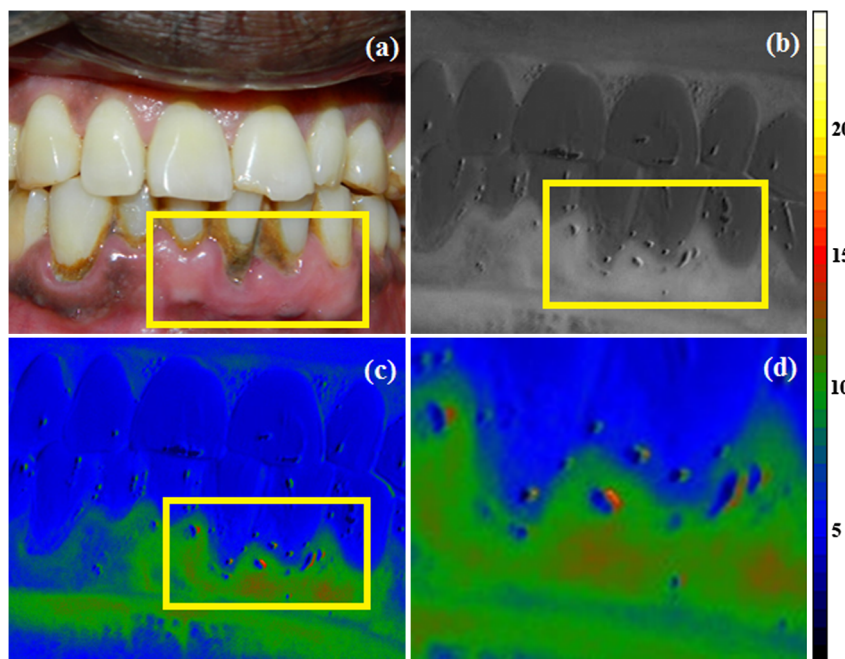


Fig. 3 (a) Gingiva with moderate inflammation highlighted inside yellow rectangle, (b) grayscale image ratio R620/R575, (c) PCM image ratio, and (d) enlarged view showing disease-active sites.

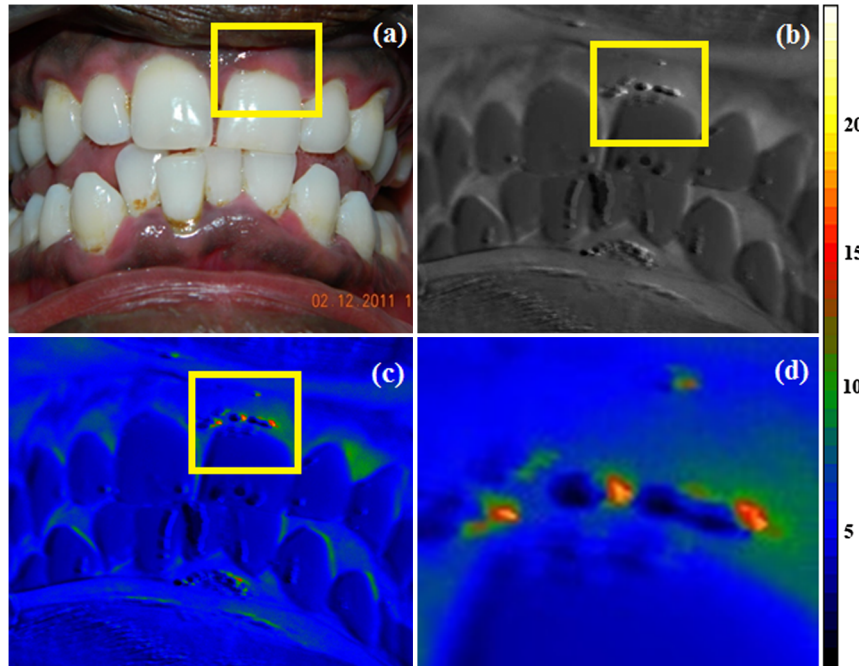


Fig. 4 (a) Gingiva with severe inflammation highlighted inside yellow rectangle, (b) grayscale image ratio R620/R575, (c) PCM image ratio, and (d) enlarged view of disease-active sites.

for mild inflammation. Figure 3(a) shows the clinical picture of a moderately inflamed gingiva. The inflammatory region is shown inside the yellow rectangular box. The PCM ratio (R620/R575) image [shown in Fig. 3(c)] of an inflammatory condition shows red spots, which can be visualized in Fig. 3(d). The average pixel intensity ratio (R620/R575) obtained for moderately inflamed gingiva is 12.92 ± 2.77 . Figure 3(b) shows the grayscale image of the moderately inflamed gingiva. Figure 4(a) is a clinical picture of severe periodontal inflammation, and Fig. 4(c)

is its PCM image with the affected site highlighted inside the yellow rectangle. The highlighted region on enlargement, shown in Fig. 4(d), shows regions of yellow color with an average pixel intensity ratio (R620/R575) value of 16.64 ± 2.18 . Figure 4(b) is the monochromatic R620/R575 ratio image of diseased gingiva before PCM.

Figure 5(a) shows a photo of the gingiva of a patient with moderate bone loss in the 12 region. Figure 5(b) shows its monochrome image R620/R575 ratio, and Fig. 5(c) shows

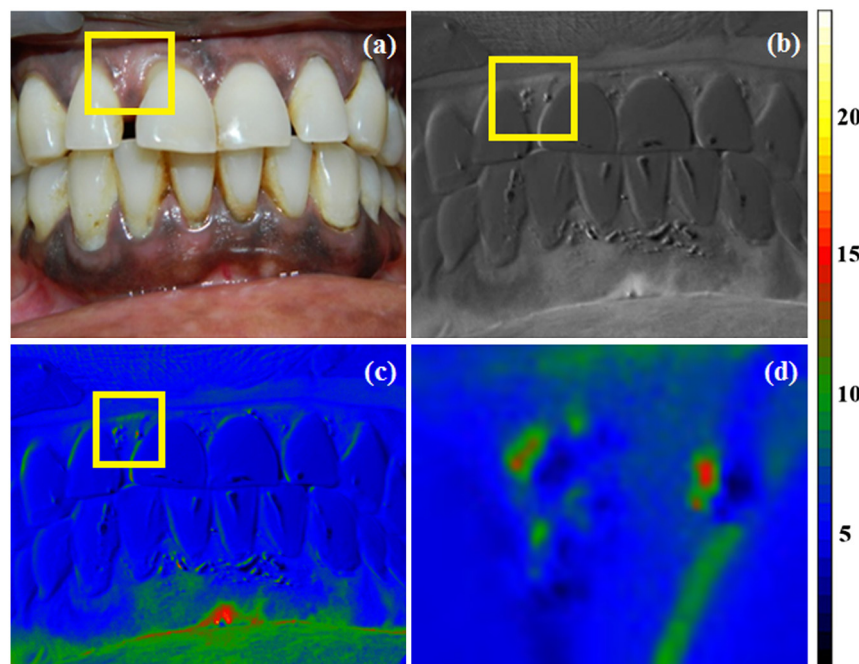


Fig. 5 Gingiva of a patient with a calculus index score of 1 and moderate bone loss in region 12: (a) Photo of the affected gingiva, (b) grayscale image ratio R620/R575, (c) PCM image ratio, and (d) enlarged view of disease-active site.

the PCM of the image ratio, with the affected region highlighted inside the yellow rectangular box. This patient had moderate periodontitis with an apparently healthy gingiva in the upper anterior sextant. The DR image correlates well with the absence of inflammation in the papillary region and inflammation in the attached gingiva in region 12, as shown in Fig. 5(d). This case was identified due to the presence of underlying inflammation in the attached gingiva analogous to periodontitis. The affected region clinically had recession and bone loss, which was confirmed through an IOPA X ray.

3.2 Scatterplot Analysis

The DR image pixel intensity ratio (R620/R575) for different categories of periodontal inflammation was determined, and a scatterplot diagram was drawn (Fig. 6). For group classification, cutoff lines are drawn in the scatterplot diagram at the mean value of the adjacent groups. For example, the average pixel intensity ratio value is 4.81 ± 1.04 for healthy tissue and 8.82 ± 1.79 for mild inflammation, so the cutoff line for discrimination between healthy and mild inflammation is drawn at the mean of 4.81 and 8.82, which is 6.81. Similarly, the cutoff lines are drawn at 10.87 and 14.78 in the scatterplot of R620/R575 ratio (Fig. 6) to discriminate between the tissue groups as mild-moderate inflammation and moderate-severe inflammation, respectively. The sensitivity and specificity obtained from the scatterplot of the R620/R575 image ratio are given in Table 3. In Fig. 6, out of 96 mild inflammatory cases, eight were misclassified as healthy, giving a sensitivity of 91.6%. Out of 77 cases of healthy gingiva, five were misclassified as mild inflammation, giving a specificity of 93%. Out of 54 cases of moderate inflammation, nine were misclassified as mild inflammation, giving a sensitivity of 83%. Out of 96 cases of mild inflammation, four were misclassified as moderate, giving a specificity of 95.8%. Similarly, out of 17 cases of severe inflammation, three were misclassified as moderate, giving a sensitivity of 82.3%. Out of 54 cases of moderately inflamed

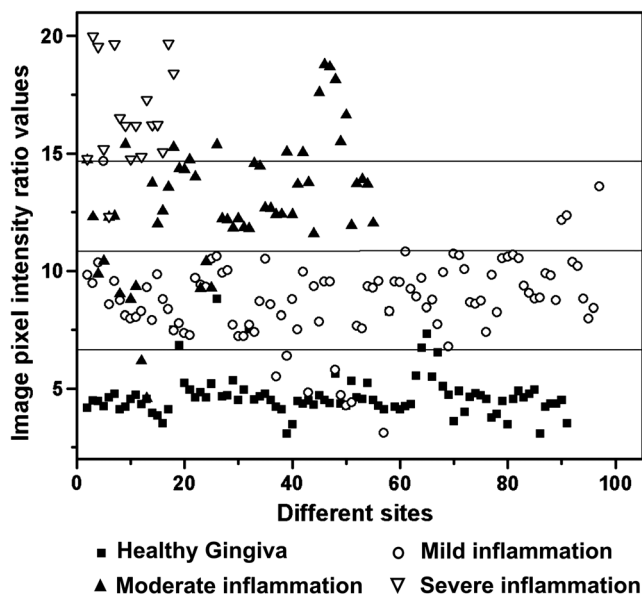


Fig. 6 Scatterplot diagram of the DR image intensity ratio R620/R575 for discrimination between healthy gingiva and mild inflammation, mild and moderate inflammation, and moderate and severe inflammation categories.

Table 3 Diagnostic accuracies obtained by DR imaging technique for the classification of gingival sites.

Diagnostic accuracy	Healthy (90)-mild (96) inflammation	Mild (96)-moderate (54) inflammation	Moderate (54)-severe (17) inflammation
Sensitivity	91.6%	83.0%	82.3%
Specificity	93.0%	95.8%	75.9%

Note: Sensitivity(Se) = TP/TP + FN, Specificity (Sp) = TN/TN + FP

gingiva, 13 were classified as severe, giving a specificity of 75.9% (Table 3).

4 Discussion

The study population comprised 15 healthy subjects, 25 subjects with gingival inflammation (test group I), and six subjects with a previous history of periodontitis and no gingival inflammation (test group II), as shown in Table 1. The sites defined as healthy in this clinical trial were from completely healthy volunteers as evaluated by a periodontist. Sites with mild and moderate inflammation in patients with severe inflammation, and sites with mild inflammation in patients with moderate inflammation, were omitted to avoid overlapping. Since periodontal breakdown is known to begin from the col, which is nonkeratinized, pixel intensity values from the ROI were taken from the papillary gingiva region in the R620/R575 ratio image. DR spectral imaging was always performed before clinical assessment of the disease stage, because clinical examinations may disturb the sites and cause bleeding, which could interfere with the measurements.

Even though only anterior sextants of the gingiva were included in this study, the average value of the pixel intensity ratio at the papillary gingival regions 13, 23, 33, and 43 did not give good correlation with BOP. This may be due to the angulation of the gingival region at these sites, since the dental arch is curved. All the other regions that were perpendicular to the look angle of the imaging camera gave good results. Therefore, in the case of healthy patients, only the data from regions 12, 21, 22, 32, 41, and 42 were included in the scatterplot. A total of 90 ROIs were obtained in the case of healthy subjects, whereas 96 ROIs of mild inflammation, 54 of moderate inflammation, and 17 of severe inflammation were included in the scatterplot diagram (Fig. 6).

4.1 DR Imaging for Monitoring of Periodontal Disease

In an earlier clinical study, it was observed that oxy-Hb concentration increases with an increase in periodontal inflammation, and the associated changes could be detected from the R620/R575 ratio with good diagnostic accuracies.²¹ In this study, the gingival erythema was monitored from changes in the intensity of oxy-Hb absorption at 575 nm in the diffusely reflected white light spectra. The results show that sites with BOP correspond well with the PCM image and the averaged pixel intensity ratio (R620/R575) value. Furthermore, it is shown that DR imaging can precisely demarcate areas with increased vascularity, which is known to occur during gingival inflammation (Figs. 2-4).

4.2 Identification of Inflammatory Changes in Subclinical Stage in Sites with Disease Activity

Periodontal destruction is site specific and does not occur in all parts of the gingiva and teeth simultaneously. The exact points of inflammation in moderately inflamed and severely inflamed gingiva, as seen in the false colored images (Figs. 3 and 4) are not observed using conventional diagnostic procedures. Therefore, DR imaging can identify areas with early inflammatory changes in the underlying tissues, even when the sites appear clinically healthy (Fig. 5) but are prone to disease. This enhances the prospect for site-specific treatments like photodynamic therapy to selectively target and inactivate periodonto-pathogenic bacteria.

The currently used diagnostic procedures cannot distinguish between disease-active and disease-inactive sites at any given point of time, nor can they reliably identify susceptible individuals based on disease-active and disease-inactive sites.²³ The DR image ratio (R620/R575) of the gingiva of a patient having apparently healthy gingiva in the upper anterior sextant (Fig. 5) corroborated well with the moderate bone loss detected in region 12 in the IOPA X ray (data not shown) and with areas in the papillary region where inflammation was absent. Similar changes were observed in the case of six patients having apparently healthy gingiva with alveolar bone loss that was revealed in the X ray. This implies that the DR imaging technique could be effectively utilized to diagnose underlying erythema in apparently healthy gingiva after scaling.

Conventional clinical examinations depend on alveolar bone and periodontal attachment loss. They cannot be used to predict the susceptibility to future disease progression or to dictate appropriate treatment plans.²³ At present, the only clinically available method for the prediction of progressive attachment loss or disease progression is BOP, which is not a good predictor of progressive attachment loss. However, the absence of BOP is an excellent predictor of periodontal stability.^{24,25}

4.3 Early Detection of Inflammation

The early detection of periodontal disease enhances the possibilities for appropriate treatment planning, whether it is prophylactic, medical, or surgical. The DR ratio images obtained in this study reveal the ability of this technique to help physicians detect early symptoms of gingival inflammation, whether due to mild gingivitis or attached bone loss. While radiographs reveal bone loss only after 30% to 50% of the mineral has been lost, the DR imaging technique has the potential to find early stages of mineral loss from the inflammatory conditions in gingival tissues. Also, early diagnosis and consequent treatment of periodontal disease may have a major impact on the control of other systemic infections.^{4,26} Therefore, the currently used technique of periodontal probing, which fails to monitor the initiation or progression of periodontal destruction, could be replaced by noninvasive DR imaging, which can diagnose early stages of periodontal breakdown.

4.4 Reproducibility of the Results

The DR imaging system used in this study assesses the given area of the periodontium as a whole and gives an objective result with uniform criteria for disease diagnosis, thereby increasing its reproducibility and reliability. Usually the clinical assessment of gingival inflammation is often subjective, because the

evaluation of visual parameters can vary from person to person. Previous studies have demonstrated that DR spectroscopy can be used to assess the degree of erythema and edema taking into consideration the light absorbed by particular chromophores. Kolias et al.²⁷ reported that erythema correlates well with the relative concentration of oxygenated hemoglobin. Although these findings were reported for skin, gingival tissues have a similar structure, consisting of an external layer of epithelium with an underlying layer and connective tissue, where most of the microvasculature is embedded.²⁸

4.5 Noninvasive Technique for Real-Time Diagnosis of Periodontal Disease

Image analysis using the scatterplot of the R620/R575 image ratio (Fig. 6) has shown a sensitivity of 91.6% and a specificity of 93% for the discrimination of healthy tissue from mild inflammation, along with a sensitivity of 83% and a specificity of 95.8% for the discrimination between mild and moderate inflammation. In comparison, a sensitivity of 82.3% and a specificity of 75.9% was obtained for the discrimination between moderate and severe inflammation. The misclassified cases cannot be completely attributed to the technique used; they could be due to the limitation in taking the conventional diagnostic technique as our gold standard. Also, in some cases, there could be a possibility for specularly reflected white light from saliva to overshadow the less intense backscattered light from underlying tissues. Since the diagnostic accuracies achieved are promising, studies on a random population would go a long way in establishing the reliability of this technique in the mapping of periodontal diseases.

5 Conclusions

The inflammatory responses are critical to the pathogenesis of periodontal disease. Until now, the diagnosis and classification of periodontal inflammation has been based almost entirely on traditional clinical assessments. Although various optical spectroscopy-based devices are under development, the DRIS presented in this paper appears to be a promising tool in the diagnosis of periodontitis and inflammation mapping. The attractive aspect of DR imaging is that it is totally noninvasive, real-time, and nonhazardous, and it does not impose any discomfort to patients during the procedure, because no tissue needs to be extracted. The white light source of the dental chair unit can be used for tissue illumination, which reduces the cost and enhances the applicability of the DR imaging system in a clinical environment.

In this study, using the DR image ratio R620/R575, mild inflammatory tissues could be discriminated from healthy with a sensitivity of 92% and a specificity of 93% and from moderately inflamed tissues with a sensitivity of 83% and a specificity of 96%. Moderately inflamed tissues could be discriminated from severe inflammation with a sensitivity 82% and a specificity of 76%. A study on six patients having a history of periodontitis sites with no overt signs of gingival inflammation showed that underlying inflammation due to the presence of plaque located deep inside the subgingival pockets could also be detected from the DR image ratio R620/R575.

The ability to detect initial inflammatory changes and to demarcate areas with underlying inflammation is an attractive feature of the DR imaging technique. However, the major limitation was that the DRIS instrument could capture images only from the upper and lower anterior sextant of the dental arch that

were almost at a right angle to the camera. As we go posteriorly toward the premolars and molars, the dental arch morphology and the angulations of the teeth change, becoming pronounced at the inner aspects of dental arch, such as the palatal aspect in the upper arch and the lingual aspect in the lower arch. Access to such inner regions can be gained by using suitable optical fibers to guide white light to the tissues and fiber bundles for imaging of the diffusely reflected light. Further studies are envisaged on a larger population with imaging fiber-coupled DRIS to explore the applicability of the DR ratio technique for noninvasive screening of periodontitis and to improve the diagnostic accuracies for discrimination of gingival inflammation.

Acknowledgments

This project was carried out as part of an Indo-Bulgarian collaborative project funded by the Department of Science & Technology, Government of India. The authors (CSP and UGN) are thankful to the research committee of CESS for their research fellowship grants. JIJ is thankful to Department of Biotechnology (DBT, Government of India) for her research associateship. We acknowledge Dr. Bindu R. Nayar, Department of Periodontics, GDC, for very fruitful discussions on various aspects of the study. We are also thankful to the postgraduate students of the GDC for their kind cooperation and help.

References

1. S. Offenbacher et al., "Periodontal infections as a possible risk factor for preterm low birth weight," *J. Periodontol.* **67**, 1103–1113 (1996).
2. F. A. Scannapieco and M. P. Rethman, "The relationship between periodontal diseases and respiratory diseases," *Dent. Today* **22**(8), 79–83 (2003).
3. F. A. Scannapieco, R. B. Bush, and S. Paju, "Associations between periodontal disease and risk for atherosclerosis, cardiovascular disease, and stroke: a systemic review," *Ann. Periodontol.* **8**(1), 38–53 (2003).
4. A. Saremi et al., "Periodontal disease and mortality in type 2 diabetes," *Diabetes Care* **28**(1), 27–32 (2005).
5. P. N. Papapanou, "Periodontal Diseases: Epidemiology," *Ann. Periodontol.* **1**(1), 1–36 (1996).
6. R. C. Page and K. S. Kornman, "The pathogenesis of human periodontitis: An introduction," *Periodontol.* **2000** **14**, 9–11 (1997).
7. S. Offenbacher, "Periodontal diseases: pathogenesis," *Ann. Periodontol.* **1**(1), 821–878 (1996).
8. M. A. Taubman, T. Kawai, and X. Han, "The new concept of periodontal disease pathogenesis requires new and novel therapeutic strategies," *J. Clin. Periodontol.* **34**(5), 367–369 (2007).
9. N. Subhash et al., "Oral cancer detection using diffuse reflectance spectral ratio R540/R575 of oxygenated hemoglobin bands," *J. Biomed. Opt.* **11**(1), 14018 (2006).
10. R. J. Mallia et al., "Oxygenated hemoglobin diffuse reflectance ratio for *in vivo* detection of oral pre-cancer," *J. Biomed. Opt.* **13**(4), 041306 (2008).
11. R.J. Mallia et al., "Diffuse reflection spectroscopy: an alternative to autofluorescence spectroscopy in tongue cancer detection," *App. Spect.* **64**(4), 409–418 (2010).
12. J. L. Jayanthi et al., "Diffuse reflectance spectroscopy: diagnostic accuracy of a non-invasive screening technique for early detection of malignant changes in the oral cavity," *BMJ open* **1**(1), e000071 (2011).
13. T. Hanioka et al., "Haemoglobin concentration and oxygen saturation in dog gingiva with experimentally induced periodontitis," *Arch. Oral Biol.* **34**(8), 657–663 (1989).
14. T. Hanioka, S. Shizukuishi, and A. Tsunemitsu, "Hemoglobin concentration and oxygen saturation of clinically healthy and inflamed gingiva in human subjects," *J. Periodontal Res.* **25**(2), 93–98 (1990).
15. G. Zonios, J. Bykowski, and N. Kollias, "Skin melanin, hemoglobin and light scattering properties can be quantitatively assessed *in vivo* using diffuse reflectance spectroscopy," *J. Invest. Dermatol.* **117**(6), 1452–1457 (2001).
16. G. N. Stamatas and N. Kollias, "Blood stasis contributions to the perception of skin pigmentation," *J. Biomed. Opt.* **9**(2), 315–322 (2004).
17. D. L. Farkas and D. Becker, "Applications of spectral imaging: detection and analysis of human melanoma and its precursors," *Pigment Cell Res.* **14**(1), 2–8 (2001).
18. K. Z. Liu, X. M. Xiang, and A. Man, "*In vivo* determination of multiple indices of periodontal inflammation by optical spectroscopy," *J. Periodontal. Res.* **44**(1), 117–124 (2009).
19. Z. Ge et al., "Assessment of local Hemodynamics in Periodontal inflammation using optical spectroscopy," *J. Periodontol.* **82**(8), 1161–1168 (2011).
20. C. Zakian et al., "*In vivo* quantification of gingival inflammation using spectral imaging," *J. Biomed. Opt.* **13**(5), 054045 (2008).
21. P. C. Sekhar et al., "Discrimination of periodontal diseases using diffuse reflectance spectral intensity ratios," *J. Biomed. Opt.* **17**(2), 027001 (2012).
22. G. C. Armitage, "Research, Science and Therapy Committee of the American Academy of Periodontology. Diagnosis of periodontal diseases," *J. Periodontol.* **74**(8), 1237–1247 (2003).
23. X. Xiang et al., "An update on novel non-invasive approaches for periodontal diagnosis," *J. Periodontol.* **81**(2), 186–198 (2010).
24. R. G. Marks et al., "Evaluation of reliability and reproducibility of dental indices 2," *J. Clin. Periodontol.* **20**(1), 54–58 (1993).
25. S. F. McClanahan, R. D. Bartizek, and A. R. Biesbrock, "Identification and consequences of distinct Loe-Silness gingival index examiner styles for the clinical assessment of gingivitis," *J. Periodontol.* **72**(3), 383–392 (2001).
26. T. E. Van Dyke and S. Dave, "Risk factors for periodontitis," *J. Int. Acad. Periodontol.* **7**(1), 3–7 (2005).
27. N. Kollias et al., "A single parameter, oxygenated hemoglobin, can be used to quantify experimental irritant-induced inflammation," *J. Invest. Dermatol.* **104**(3), 421–424 (1995).
28. A. Nanci, *Ten Cate's Oral Histology: Development, Structure, and Function*, 6th ed., Mosby, St. Louis (2003).